

Research Article

Ma xing shi gan decoction eliminates PM2.5-induced lung injury by reducing pulmonary cell apoptosis through Akt/mTOR/p70S6K pathway in rats

Yefang Wang^{1,*}, Bo Zhao^{2,*}, Yuxiang Fei², Qiyang Yin², Jianping Zhu², Guanghui Ren², Bowen Wang², Weirong Fang² and  Yunman Li²

¹Department of Paediatrics, Nanjing Integrated Traditional Chinese and Western Medicine Hospital, Nanjing 210014, People's Republic of China; ²State Key Laboratory of Natural Medicines, School of Basic Medicine and Clinical Pharmacy, China Pharmaceutical University, Nanjing 210009, People's Republic of China

Correspondence: Bo Zhao (532045956@qq.com) or Weirong Fang (weirongfang@cpu.edu.cn) or Yunman Li (yunmanlicpu@163.com)



The present study was designed to investigate the anti-apoptosis effect of Ma xing shi gan decoction (MXD) on PM2.5-induced lung injury via protein kinase B (Akt)/mTOR/p70S6K pathway. A UPLC-MS/MS system was introduced for component analysis of MXD. Rats were instilled with PM2.5 solution suspension intratracheally to induce acute lung injury. The rats were then orally administered with MXD (16, 8, and 4 g/kg) once a day for 7 consecutive days. The therapeutic effects of MXD were evaluated by Hematoxylin and Eosin (HE) staining. The apoptotic cell death was analyzed by terminal-deoxynucleotidyl transferase-mediated nick-end labeling (TUNEL) assay. The alterations in cytochrome c (Cytc) and cleaved-caspase-3 (C-caspase-3) were measured by immunohistochemistry (IHC). The expressions of Bax, B-cell lymphoma 2 (Bcl-2), p-Akt, p-mTOR and p-p70S6K were detected by Western blot. *In vitro*, PM2.5 exposure model was introduced in A549 cell, followed by incubation with MXD-medicated serum. Hoechst staining was used to determine apoptotic rate. The levels of Bax, Bcl-2, p-Akt, p-mTOR and p-p70S6K were detected by Western blot. Our results *in vivo* indicated that treatment with MXD decreased histopathological changes score, TUNEL-positive cells rate, expressions of Cytc and C-caspase-3. The *in vitro* results revealed that incubation with MXD-mediated serum decreased apoptotic rate. Both results *in vivo* and *in vitro* demonstrated that MXD inhibited pro-apoptotic protein Bax and promoted anti-apoptotic protein Bcl-2 expression. Likewise, MXD activated Akt/mTOR/p70S6K signal pathway, which was also confirmed by Western immunoblotting. In conclusion, MXD attenuates lung injury and the underlying mechanisms may relate to regulating the apoptosis via Akt/mTOR/p70S6K signaling pathway activation.

*These authors contributed equally to this work and should be considered as co-first authors.

Received: 29 October 2019
Revised: 02 July 2020
Accepted: 03 July 2020

Accepted Manuscript online:
06 July 2020
Version of Record published:
09 July 2020

Introduction

Fine particulate matter (PM2.5) refers to particulate matter with an aerodynamic equivalent diameter of 2.5 microns or less in air. It can be suspended in the air for a long time, and the higher its concentration in the air, the more serious the air pollution will be [1]. Epidemiological studies demonstrate that PM2.5 exposure is closely related to respiratory diseases. Particles with a diameter of 10 µm are usually deposited in the upper respiratory tract, but particles with diameter less than 2.5 µm can penetrate deep into the bronchioles and alveoli. When PM2.5 enters the alveoli, it can directly affect the ventilation function of the lungs and cause lung injury [2]. With the development of industrialization, the concentration of PM2.5 in air is increasing year by year [3]. Long-term exposure to PM2.5 poses a great threat to human health, which has been confirmed by *in vivo* experiments. He et al. pointed out PM2.5 exposure causes oxidative

Table 1 The composition of MXD

English name	Latin name	Chinese name	Proportion (g)
Ephedra Herb	<i>Ephedra sinica</i> Stapf	Ma huang	4
Bitter Almond	<i>Armeniaca Amarum</i> Semen	Ku xing ren	12
Gypsum	<i>Gypsum fibrosum</i>	Shi gao	24
Liquorice Root	<i>Glycyrrhiza uralensis</i> Fisch	Gan cao	8

stress-dependent inflammation in lungs which are rich in type II alveolar cells [4]. Meanwhile, a study suggested that PM2.5 induces cell apoptosis in human lung alveolar epithelial (A549) cells [5].

Apoptosis plays a crucial role in the pathogenesis and development of many respiratory diseases such as pneumonia and asthma, which is regulated by multiple pathways [6]. When PM2.5 stimulates the respiratory tract, PM2.5 detained in the bronchi and alveoli can cause damage or even death of the lung epithelial cells [7]. As the injury progresses, excessive apoptosis plays an important role in lung cell death, but the effective intervention remains to be explored.

With a long history and extensive clinical practice, the role of Chinese medicine in the treatment of some diseases attracted much attention [8]. Ma xing shi gan decoction (MXD) comprises the monarch drug Ephedra Herb, the minister drug Gypsum, the assistant drug Bitter Almond, and the guide drug Liquorice Root. As a classic famous prescription in *Treatise on Febrile Diseases*, it is able to treat lung diseases such as upper respiratory tract infection, acute bronchitis, pneumonia and bronchial asthma. It has shown an excellent safety and efficacy record for thousands of years. MXD has been reported to inhibit the expression of inflammatory factor expression in lung tissue induced by influenza virus A H1NI, and the terminal-deoxynucleotidyl transferase-mediated nick-end labeling (TUNEL) assay demonstrates the protection of MXD in lung tissue [9]. However, in recent years, few studies have reported the effect of MXD against PM2.5-induced lung injury at the perspective of anti-apoptosis.

The aim of the present study was to investigate the effect of MXD in attenuating PM2.5-induced lung injury and explore the underlying mechanism. Our results will provide a theoretical and practical basis for the treatment of PM2.5-induced lung injury.

Materials and methods

Experimental drugs and reagents

PM2.5 collected from January to May 2018 in suburb of Nanjing was kindly provided by Nanjing Environmental Monitoring Center. After sterilization under ultraviolet radiation for 1 h, the concentration of PM2.5 suspension was adjusted to 10 mg/ml with deionized water. Before use, the suspension was fully suspended to avoid agglomeration.

All crude drugs were purchased by the pharmacy of Nanjing Integrated Traditional Chinese and Western Medicine Hospital and identified as authentic by Yong Wang (Professor, Nanjing Integrated Traditional Chinese and Western Medicine Hospital, China).

The composition and doses of MXD have been listed in Table 1. Ephedra Herb (Sanyue Traditional Chinese Medicine Co., Ltd, Nantong, China) was decocted in 1 l of double distilled water for 1 h. After skimming the scum, Bitter Almond (Jiangsu Huahong Pharmaceutical Technology Co., Ltd, Danyang, China), Gypsum (Jiangsu Huahong Pharmaceutical Technology Co., Ltd, Danyang, China) and Liquorice Root (Hangzhou Zhende Traditional Chinese Medicine Co., Ltd, Hangzhou, China) were added and boiled for 40 min. After that the extract was filtered and enriched by rotary evaporation. The crude drug concentration of MXD was 2 g/ml. For drug administration at different doses, MXD was diluted using normal saline.

Quantitative analysis of MXD by ultra-performance liquid chromatography-tandem mass spectrometry/mass spectrometry

Standards of Ephedrine hydrochloride (CAS No. 50-98-6, purity 100.0%) and pseudoephedrine hydrochloride (CAS No. 345-78-8, purity 99.8%) were purchased from National Institutes for Food and Drug Control. Standards of Liquiritin (CAS No. 551-15-5, purity \geq 98%), Glycyrrhizic acid ammonium salt (CAS No. 53956-04-0, purity \geq 98%) and Amygdalin (CAS No. 29883-15-6, purity \geq 98%) were purchased from Solarbio Science and Technology Co., Ltd., Beijing, China.

Table 2 Elution condition for preliminary UPLC-MS analysis

Time (min)	MP A%	MP B%	Flow rate (ml/min)
Initial	98.0	2.0	
2.00	98.0	2.0	
2.40	70.0	30.0	
8.00	5.0	95.0	0.400
9.00	5.0	95.0	
9.20	98.0	2.0	
10.00	98.0	2.0	

The main chemical components of MXD were revealed by ultra-performance liquid chromatography-tandem mass spectrometry/mass spectrometry (UPLC-MS/MS). MXD was diluted 10000-times with 50% (v/v) methanol in water. The test solution was obtained after filtration.

The reference standard samples (ephedrine hydrochloride, pseudoephedrine hydrochloride, liquiritin, glycyrrhizic acid ammonium salt and amygdalin) were weighed accurately and dissolved in 50% (v/v) methanol in water at a concentration of 1 mg/ml. After diluting and pooling, the mixed reference standard solution containing ephedrine hydrochloride (500 ng/ml), pseudoephedrine hydrochloride (500 ng/ml), liquiritin (500 ng/ml), glycyrrhizic acid ammonium salt (500 ng/ml) and amygdalin (500 ng/ml) was obtained.

The preliminary analysis was performed using an Acquity UPLC BEH C18 (2.1 × 50 mm, 1.7 μm) column in both positive and negative electrospray ionization mode. For positive electrospray ionization mode, mobile phase solvent A consisted of aqueous phase of ammonium acetate (5 mmol/l), and mobile phase solvent B was pure methanol. The common elution condition is shown in Table 2.

Animals and grouping

Male Sprague–Dawley rats (200–250 g) were purchased from Qinglongshan Animal Farm of Nanjing (Nanjing, China, license number: SCXK (Su) 2019-0001). All the experiments took place in the China Pharmaceutical University (Nanjing, China). Animals were used after 7-day acclimation. All animals were maintained under standard environment conditions (23 ± 2°C, 55 ± 5% humidity and 12-h/12-h light/dark cycle). All animals were allowed free access to tap water and standard laboratory rat food. All animal studies were in accordance with the National Institute of Health (NIH) guidelines for the Care and Use of Laboratory Animals approved by the Animal Ethics Committee of China Pharmaceutical University. All efforts were made to minimize animal suffering.

Rats were randomly divided into six groups: control group, intervention group, PM2.5-stimulated group, MXD (16 g/kg) group, MXD (8 g/kg) group, MXD (4 g/kg) group. In order to verify whether MXD interferes with normal rats, an intervention group was introduced. The middle dose of MXD was chosen on the basis of human clinical dose (1.3 g/kg) × 6.3 (conversion coefficient between rat and human) [10]. Two hours after the last PM2.5 suspension instillation, rats were intragastrically administered with MXD in different dosages at the volume of 1 ml/100 g for 7 consecutive days. Rats in intervention group were treated with MXD at the dose of 16 g/kg. Rats in control group and PM2.5-stimulated group were administered with the same volume of normal saline.

Surgical procedure of PM2.5-induced model and drug treatment

Rats were anesthetized with 3% isoflurane in O₂ for 40 min with a respirator mask, fixed in the supine position and tilted to an angle of 45° to horizontal plane. Then the fixed device was placed on a shaking table (vacillating to the left and right). Acute lung injury was then induced by PM2.5 instillation. Briefly, the rat's trachea was inserted by a trocar (0.6 mm in inner diameter), followed by PM2.5 suspension injection into the trachea through the trocar at a volume of 0.1 ml/100 g body weight. Then the shaking table was turned on to rolled rats gently 60 s (at the speed of 30 cycles per minute) for distributing PM2.5 suspension equally in both lungs. This operation was done at the first, third, fifth and seventh days. Two hours after the last instillation of PM2.5 suspension, MXD was administered as described in section "Animals and grouping". Rats in control group received tracheal intubation except for PM2.5 instillation.

Tissue preparation

Two hours after the last administration, rats were killed by intravenous injection of pentobarbital (100 mg/kg), followed by perfusion with 50 ml normal saline, after which lungs were rapidly removed and fixed in 4% paraformaldehyde for 24 h. The lungs were then immersed in a 30% sucrose solution in PBS and stored at 4°C until section cutting. Lungs were embedded in paraffin and sliced into sections with 4-micron-thickness.

Hematoxylin and Eosin staining

Sections of paraffin-embedded tissue were subjected to Hematoxylin and Eosin (HE) staining to estimate damage situation of alveolar and peribronchial lesions as described previously [11]. The histopathological changes of lung tissues were then observed with the optical microscope (Olympus BX53; Japan). The degree of lung injury was graded on a scale of 0–4 (0, absent; 1, light; 2, moderate; 3, strong; 4, intense) which was based on alveolar septal thickening, proteinaceous debris, neutrophils infiltration and other histologic features [12].

Immunohistochemistry

The paraffin sections were subjected to immunohistochemical staining to quantify the expression of Cytochrome *c* (Cyt c) and cleaved-caspase-3 (C-caspase-3), two main effector proteins during apoptosis. The sections were blocked with 10% normal goat serum, and incubated overnight with primary antibody to Cyt c (Servicebio, China, 1:1000) and C-caspase-3 (servicebio, China, 1:1000) at 4°C. After washing with PBS for three times, sections were exposed to the secondary antibody at 37°C for 20 min, and then visualized using 0.05% 3,3'-diaminobenzidine-solution (DAB) [13]. The signal intensity of immunoreactivity was semiquantitatively evaluated using H-score analysis according to a previous study. The sections were then counterstained using Hematoxylin, rinsed with 1% hydrochloric acid alcohol, cleared in xylene and mounted. The expression of Cyt c and C-caspase-3 was evaluated using the optical microscope in areas chosen randomly. The results were analyzed using ImageJ 1.50i (National Institutes of Health, U.S.A.).

TUNEL assay

To examine the protection of MXD on apoptotic cell death after exposure to PM_{2.5}, TUNEL assay was conducted according to previously published methods [14]. The paraffin sections were incubated with the TUNEL assay kit reagents for 1 h at 37°C after blockage and permeabilization. Sections were counterstained with DAPI. The slides were photographed using fluorescence microscope (Nikon Eclipse Ti-SR; Japan) and the images were analyzed using ImageJ 1.50i.

Preparation of MXD-medicated serum

Five rats (250–280 g) were intragastrically administrated with MXD at 16g/kg for 7 days. Then blood samples were obtained from the arteria carotis communis, followed by centrifugation at 3000×*g* for 10 min and inactivation at 56°C water bath for 30 min. Then the serum was filtered through a filter having a pore size of 0.22 microns, pooled and stored at –80°C for further use. Another five rats were administered with equal volume of normal saline, the nonimmune serum was collected and handled as described above, and used as control serum. The MXD-medicated serum was diluted by Dulbecco's modified Eagle's medium (DMEM) at various concentrations (volume fractions): 20% medicated serum; 10% medicated serum + 10% nonimmune serum; 5% medicated serum + 15% nonimmune serum. The quantification of main ingredients of interest in the medicated serum are shown in Supplementary Materials.

Cell culture and PM_{2.5} stimulation

A549 cells, a human alveolar basal epithelial cell line, was purchased from American Type Culture Collection (ATCC) and cultured in DMEM with 10% fetal bovine serum, 5% CO₂ and 95% O₂ at 37°C. The cells were digested and passaged every 1 or 2 days.

Cells were seeded in 96-well plates at the density of 5 × 10³ cells/well and cultured overnight. Then, cells were randomly divided into six groups: control group, intervention group, PM_{2.5}-exposed group and three treatment groups. The A549 cells in control group were incubated with nonimmune serum 20% for 24 h. Cells in intervention group were incubated with MXD-medicated serum at the volume fraction of 20% for 24 h. Cells in PM_{2.5} group were stimulated with PM_{2.5} suspension at the concentration of 20 μg/cm² for 24 h. Cells in the treatment groups were incubated with various concentrations (volume fractions) of MXD-medicated serum (20% medicated serum; 10% medicated serum + 10% nonimmune serum; 5% medicated serum + 15% nonimmune serum) right after the addition of PM_{2.5}

for 24 h. The PM_{2.5} concentration and incubation time were determined by previous study (data not shown). The total volume fractions of serum in all groups were strictly adjusted to 20% for uniformity.

Cell viability assay

Cells were incubated with different concentrations (20, 10, 5%) of MXD-medicated serum to assess the cytotoxicity of MXD-medicated serum. To preliminarily evaluate the protection of MXD-medicated serum against PM_{2.5} challenge, 24 h after the incubation of medicated serum and PM_{2.5}, 20 μ l MTT solution (5 mg/ml) was added to each well followed by incubation for another 4 h at 37°C in darkness. Supernatant of medium containing MTT was carefully removed, and the black-purple crystals were dissolved by 200 μ l DMSO. After a 10-min shaking, the absorbance was measured at 570 nm using a microplate reader (Thermo Multiskan FC, U.S.A.).

Hoechst staining

The apoptotic cells were analyzed by Hoechst staining as previously described [15]. Briefly, 24 h after the induction of MXD-medicated serum and PM_{2.5}, cells were incubated with Hoechst 33258 (Wanleibio, China) at room temperature for 10 min. After washing with PBS for three times (5 min per time), the images were captured under a fluorescence microscope (Olympus IX53; Japan).

Western blot

Lung tissues and cells were lysed conventionally using the RIPA lysis buffer containing a mixture of PMSF and phosphatase inhibitor (v/v = 97:1:2) separately on ice. The total protein concentration was determined by bicinchoninic acid (BCA) protein assay. Equal amount of proteins was subjected to 10% SDS/PAGE and transferred on to polyvinylidene fluoride (PVDF) membranes [16]. After the transfer, the blots were blocked with 5% skimmed milk for 2h and incubated overnight with diluted primary antibody B-cell lymphoma 2 (Bcl-2; Wanleibio, 1:500), Bax (Abways, 1:1000), β -actin (Abways, China, 1:3000), protein kinase B (Akt/PKB; Wanleibio, 1:500), phospho-Akt (Ser⁴⁷³, Wanleibio, 1:500), phospho-mTOR (Ser²⁴⁴⁸, Wanleibio, 1:500), mTOR (Wanleibio, 1:500), phospho-p70S6k (Thr³⁸⁹, Cell Signaling Technology, 1:500), p70S6k (Cell Signaling Technology, 1:1000). After washing with PBS (10 min \times 3-times), bands were incubated with horseradish peroxidase (HRP)-conjugated anti-rabbit IgG (Abways, China, 1:5000) for 2 h at room temperature. The blots were then developed using enhanced chemiluminescence (ECL) solution (Applygen Technologies Inc.). The semi-quantitative analysis was performed using densitometry analysis by ImageJ 1.50i.

Statistical analysis

All data are expressed as means \pm S.D. Statistical analysis was performed using SPSS 22.0 statistical software (IBM Corp, U.S.A.) by one-way analysis of variance (ANOVA), followed by LSD post-hoc test (homogeneity of variance) and Games–Howell post-hoc test (heterogeneity of variance). A value of $P < 0.05$ was considered as statistically significant.

Results

Chemical standardization of MXD by UPLC-MS/MS

The MXD was analyzed using UPLC–MS/MS to quantify the main ingredients and obtain the chemical profile. Mass spectrometry was acquired in positive and negative electrospray ionization modes. Five major components (Figure 1A) were identified in MXD sample. A positive electrospray ionization mode LC-MS profile was developed for MXD sample and mixed standard solution (Figure 1B,C), and the result confirmed the presence of ephedrine hydrochloride, pseudoephedrine hydrochloride, liquiritin and glycyrrhizic acid in MXD. Besides, a negative electrospray ionization mode LC-MS profile was developed for MXD sample and mixed standard solution (Figure 1D,E), and the result confirmed the presence of amygdalin, liquiritin and glycyrrhizic acid in MXD.

Therapeutic effects of MXD on lung injury in PM_{2.5}-stimulated rats

Acute lung injury model was established in rats to investigate the protective effects of MXD against PM_{2.5}-induced lung injury. The lungs of rats exposed to PM_{2.5} exhibited a significant degree of damage with obvious swell, congestion and blood spots (Figure 2A). Significant pathological changes, including alveolar wall thickening, pulmonary interstitial edema and inflammatory cell infiltration were observed in the lung tissues of PM_{2.5}-stimulated rats (Figure 2B). Histological examination showed that lung injury score in PM_{2.5}-stimulated group was markedly increased compared with the control group and intervention group ($P < 0.01$). Treatment with MXD (16 and 8 g/kg) for 7 consecutive days

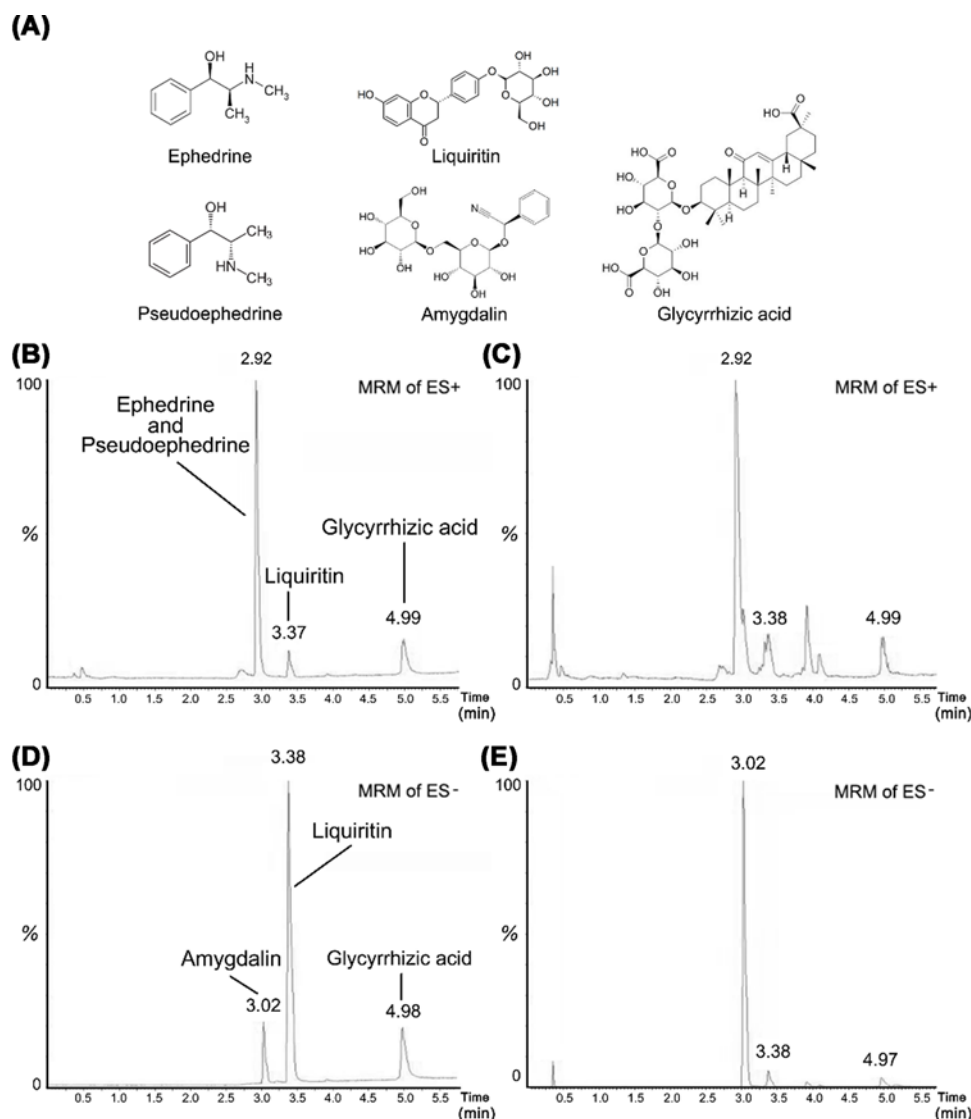


Figure 1. Chemical structures of the five major components in MXD and representative chromatograms of mixed standard solution and sample

(A) Chemical structures of the five major components in MXD. Representative chromatograms of standard solution (B) and MXD sample (C) in positive electrospray ionization mode. Representative chromatograms of standard solution (D) and MXD sample (E) in negative electrospray ionization mode. The corresponding relation between chromatographic peaks and compounds are shown in the figures.

significantly attenuated the histopathological changes induced by PM_{2.5} (Figure 2A,B). In addition, damage scores in the 16 and 8 g/kg MXD groups were significantly lower than that in PM_{2.5}-stimulated group ($P < 0.01$, Figure 2C). These results preliminarily demonstrated that treatment with MXD attenuates lung injury in PM_{2.5}-stimulated rats.

MXD treatment inhibits pulmonary cell apoptosis in PM_{2.5}-stimulated rats

For investigating the effects of MXD on pulmonary cell apoptosis after PM_{2.5} challenge, TUNEL assay was conducted in rat lung tissues. TUNEL-positive cells increased significantly in PM_{2.5}-stimulated group compared with the control group and intervention group ($P < 0.01$). Notably, compared with the PM_{2.5}-stimulated group, the apoptosis rate of MXD-treated groups decreased significantly ($P < 0.01$), demonstrating that MXD has the ability to prevent pulmonary cell apoptosis after PM_{2.5} challenge (Figure 3).

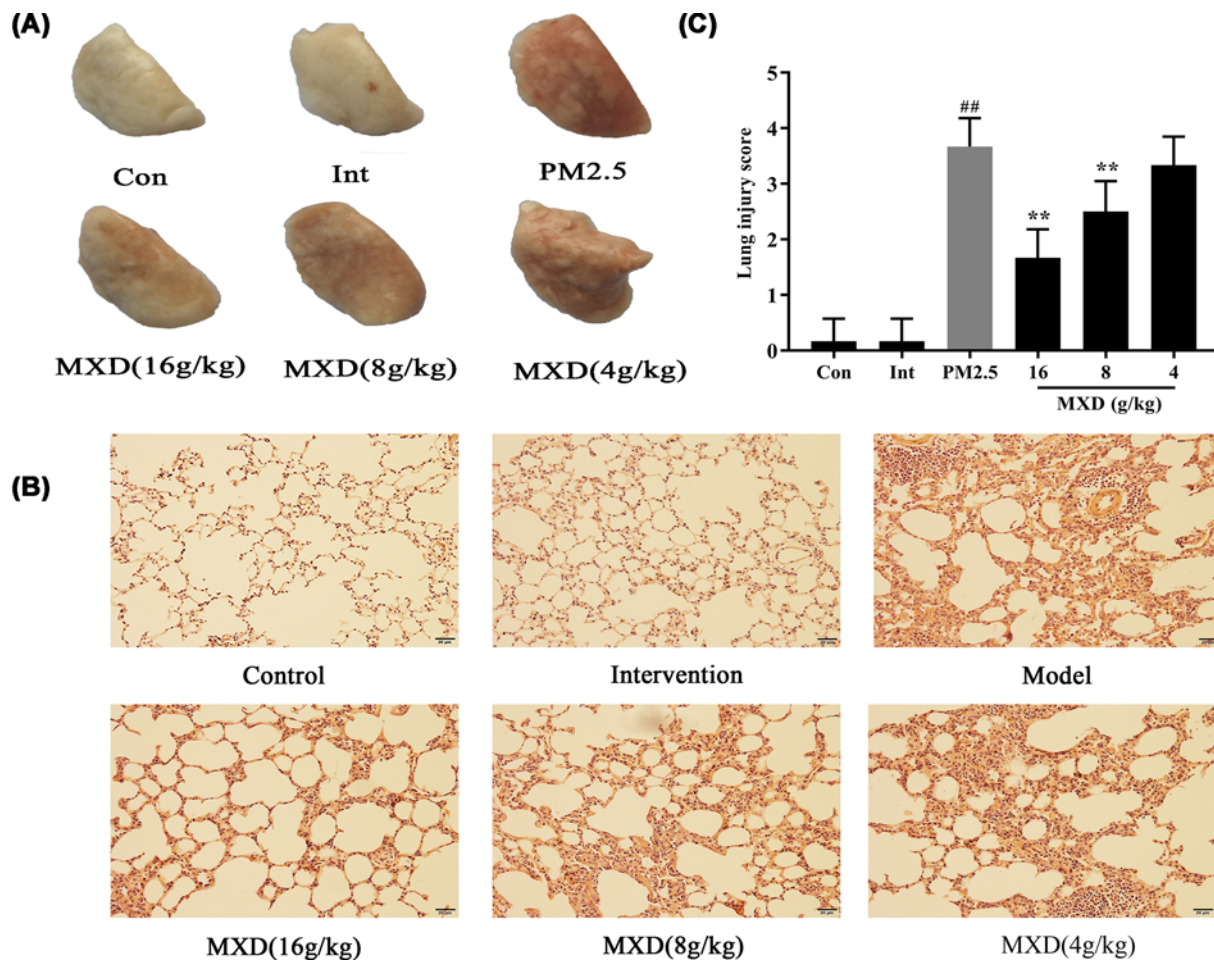


Figure 2. Therapeutic effect of MXD (16, 8, 4 g/kg) against PM2.5-induced lung injury after treatment with MXD for 7 consecutive days

The PM2.5-stimulated group, MXD treatment group underwent PM2.5 stimulation while the control group and intervention group underwent the same surgical procedure without the transtracheal instillation. (A) Observation of pathological changes in lung tissues by naked eye after normal saline infusion. (B) Representative HE staining images of rat lung tissues (magnification, $\times 200$). (C) Lung histologic injury score. Data are shown as mean \pm S.D. $n=6$ /group, ** $P<0.01$ compared with PM2.5-stimulated group; ### $P<0.01$ PM2.5-stimulated group compared with control group. Con, control group; Int, intervention group; PM2.5, PM2.5-stimulated group.

MXD down-regulated Cytc and C-caspase-3 expressions in PM2.5-stimulated rats

Cytc and C-caspase-3 are critical proteins involved in the process of apoptosis, and abnormal elevation of Cytc level may activate the caspase-3, which acts as an executioner during apoptosis. To perceive the expression of Cytc and C-caspase-3, immunohistochemistry (IHC) staining analysis was conducted after a 7-day MXD treatment. As shown in Figure 4, challenge of PM2.5 significantly increased the expression of Cytc ($P<0.01$) and C-caspase-3 ($P<0.01$) compared with the control group and intervention group. Notably, MXD (8 and 16 g/kg) suppressed the expression of Cytc ($P<0.01$) and C-caspase-3 ($P<0.01$), indicating MXD could inhibit the activation of Cytc and C-caspase-3 significantly.

MXD protected cell viability when A549 cells exposed to PM2.5

First, the viability of A549 was measured by MTT assay to explore the toxicity of MXD under our laboratory conditions. Compared with the control group, the viability of A549 in MXD-medicated serum at concentrations 20, 10, 5 and 2.5% exhibited no significant difference ($P>0.05$). Therefore, the high concentration of MXD medicated serum

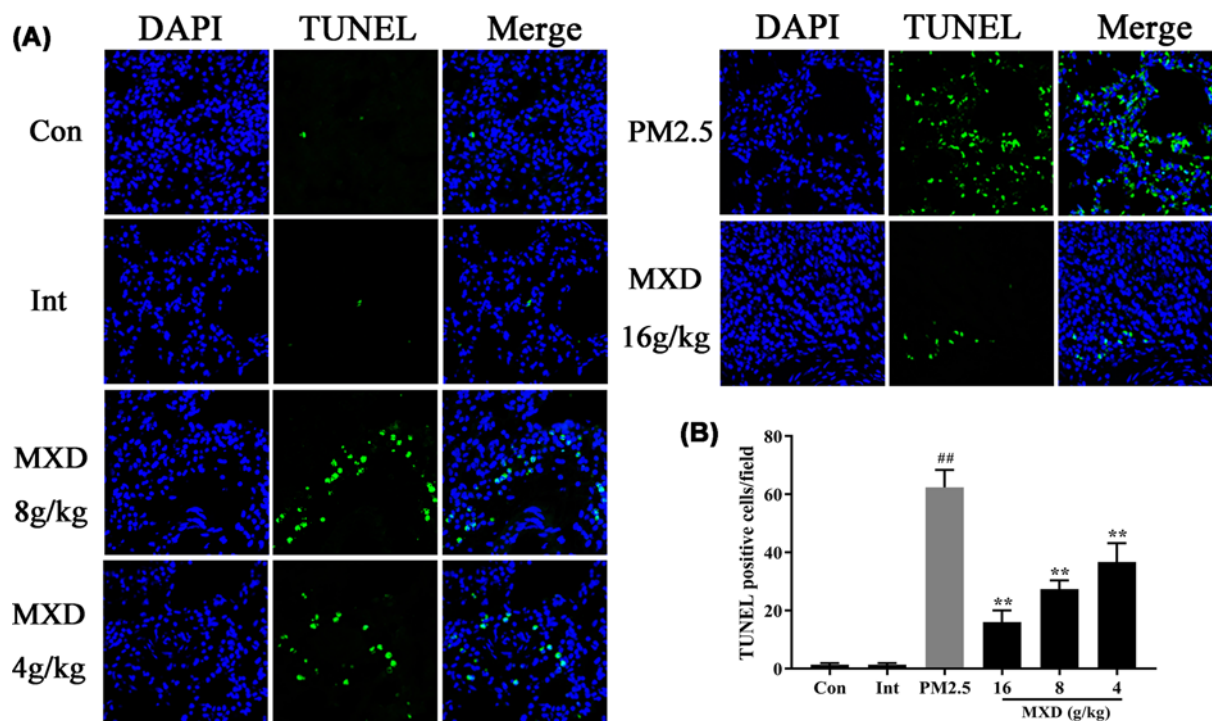


Figure 3. The effect of MXD on the number of TUNEL-positive cells in rat lung tissues after treatment with MXD for 7 consecutive days

(A) Representative images of TUNEL staining, TUNEL-positive staining (in green) and DAPI (in blue) of the rat lung tissues. TUNEL-positive cells in five fields were counted under $\times 400$ magnification. (B) Quantitative analysis of TUNEL positive cells. Data are shown as mean \pm S.D. $n=3$ /group, ** $P<0.01$ compared with PM2.5-stimulated group; ## $P<0.01$ compared with control group.

was set at 20%, and the low concentration at 5%. To quantify the main ingredient in the-medicated serum, the representative chromatograms of the five compounds in reference standard solution and medicated serum were shown in Supplementary Figure S1.

The viability of A549 cells was measured by MTT assay for preliminarily evaluating the protection of MXD-medicated serum against PM2.5 challenge. As shown in Figure 5, after PM2.5 exposure, the cell viability of A549 cells was strikingly decreased in comparison with control group and intervention group ($P<0.01$). However, after incubation with different concentrations of MXD-medicated serum, the viability of A549 cells was remarkably enhanced in comparison with PM2.5-stimulated group in a dose-dependent manner.

MXD treatment inhibits cell apoptosis when A549 cells exposed to PM2.5

Hoechst 33253 has the ability to stain the nucleus of the cells and normally applied to assess the level of apoptosis based on the specific morphological changes in nucleus during apoptosis [17]. The bright spots which indicate nuclear condensation can be observed in apoptotic cells after the exposure to PM2.5 for 24 h. However, there were no obvious apoptotic changes observed in the control group and intervention group. After incubation of MXD-medicated serum with different concentrations, the apoptotic rate was decreased significantly compared with the PM2.5-stimulated group ($P<0.01$, Figure 6).

MXD regulated Bax and Bcl-2 expressions *in vitro* and *in vivo*

The expression of Bax and Bcl-2 were further investigated both *in vivo* and *in vitro* by Western blot. As shown in Figure 7A,B, compared with the control group, PM2.5 exposure induced a significant increase in the expression of Bax and decrease in the expression of Bcl-2, *in vivo* and *in vitro* ($P<0.01$). However, treatment with MXD (16, 8 g/kg) and MXD-medicated serum (20 and 10%) significantly lowered the expression of Bax ($P<0.01$). Besides, the expression of Bcl-2 was significantly increased by MXD (16, 8 g/kg) and MXD-medicated serum (20 and 10%) in comparison with PM2.5 group ($P<0.01$, Figure 7C,D).

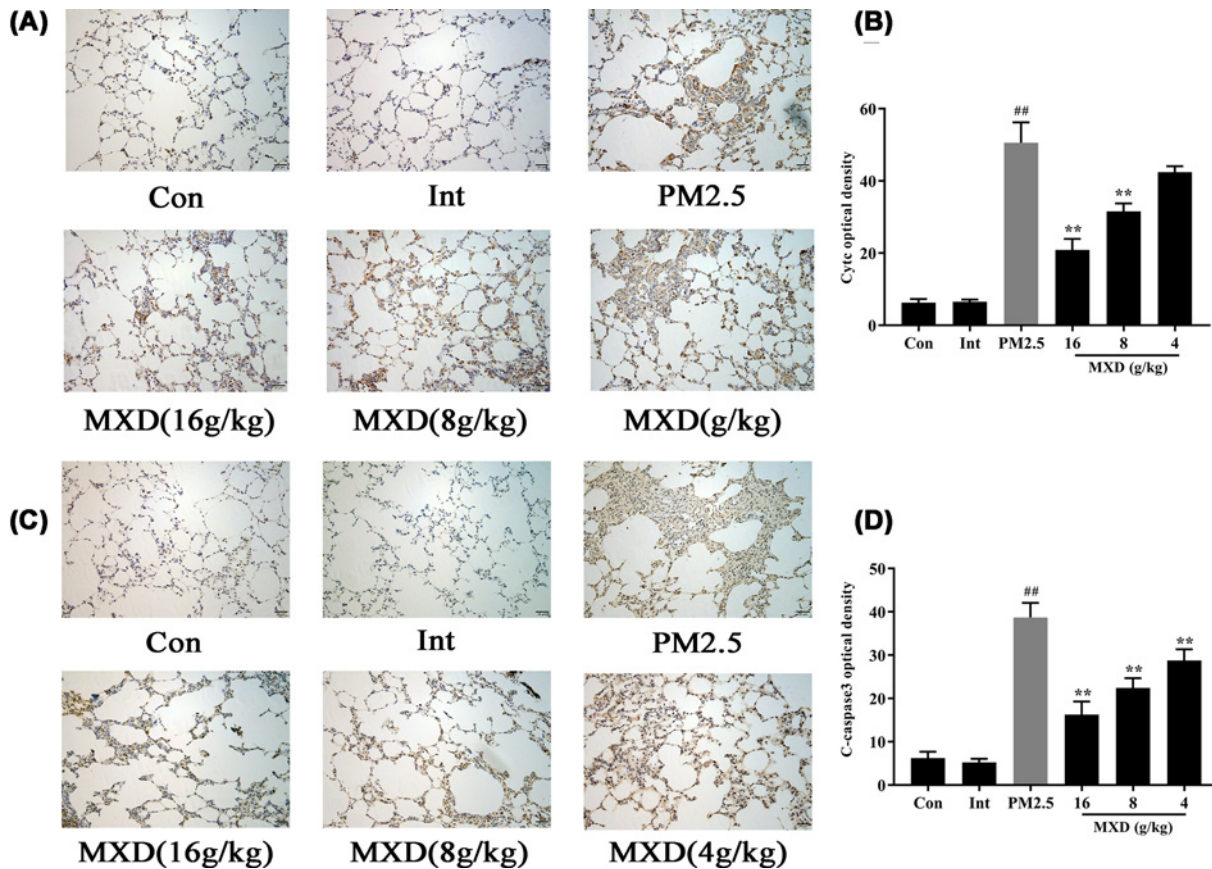


Figure 4. The effect of MXD on the expression of Cytc and C-caspase-3 in rat lung tissues after treatment for 7 consecutive days

(A) Representative images of immunohistochemical staining (magnification, $\times 200$) of Cytc in rat lungs. (B) Quantification of the positive staining (integrated optical density) of Cytc. (C) Representative images of immunohistochemical staining (magnification, $\times 200$) of C-caspase-3 in rat lungs. (D) Quantification of the positive staining (integrated optical density) of C-caspase-3. Each column represents the mean \pm S.D., $n=3$ /group, $**P<0.01$ compared with PM2.5-stimulated group; $##P<0.01$ compared with control group.

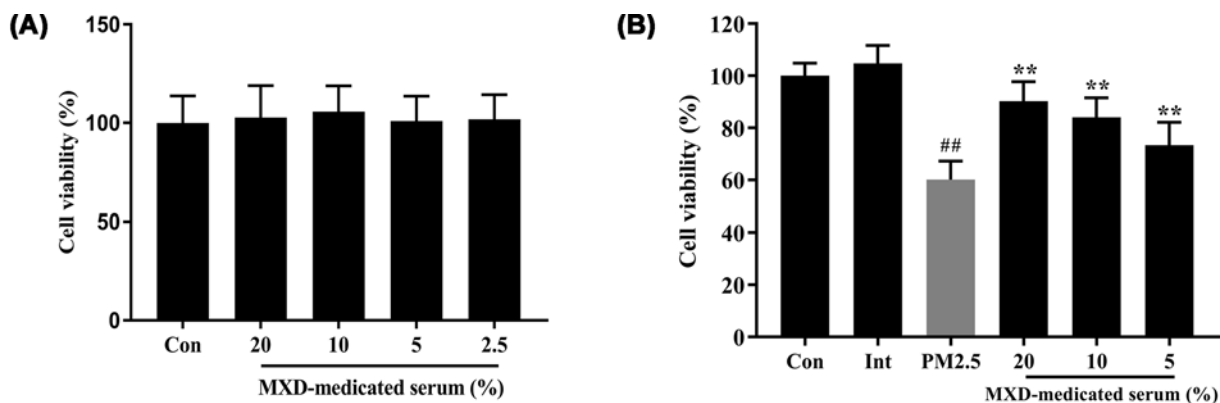


Figure 5. Effect of MXD-mediated serum on the cell viability of A549 cells after a 24-h incubation

(A) The cytotoxic effects of different concentrations of MXD-mediated serum. (B) Except the control group and intervention group, the PM2.5-stimulated group, MXD group were treated with the intervention of PM2.5. Data are shown as mean \pm S.D. $n=8$ /group, $**P<0.01$ compared with PM2.5-stimulated group; $##P<0.01$ compared with control group.

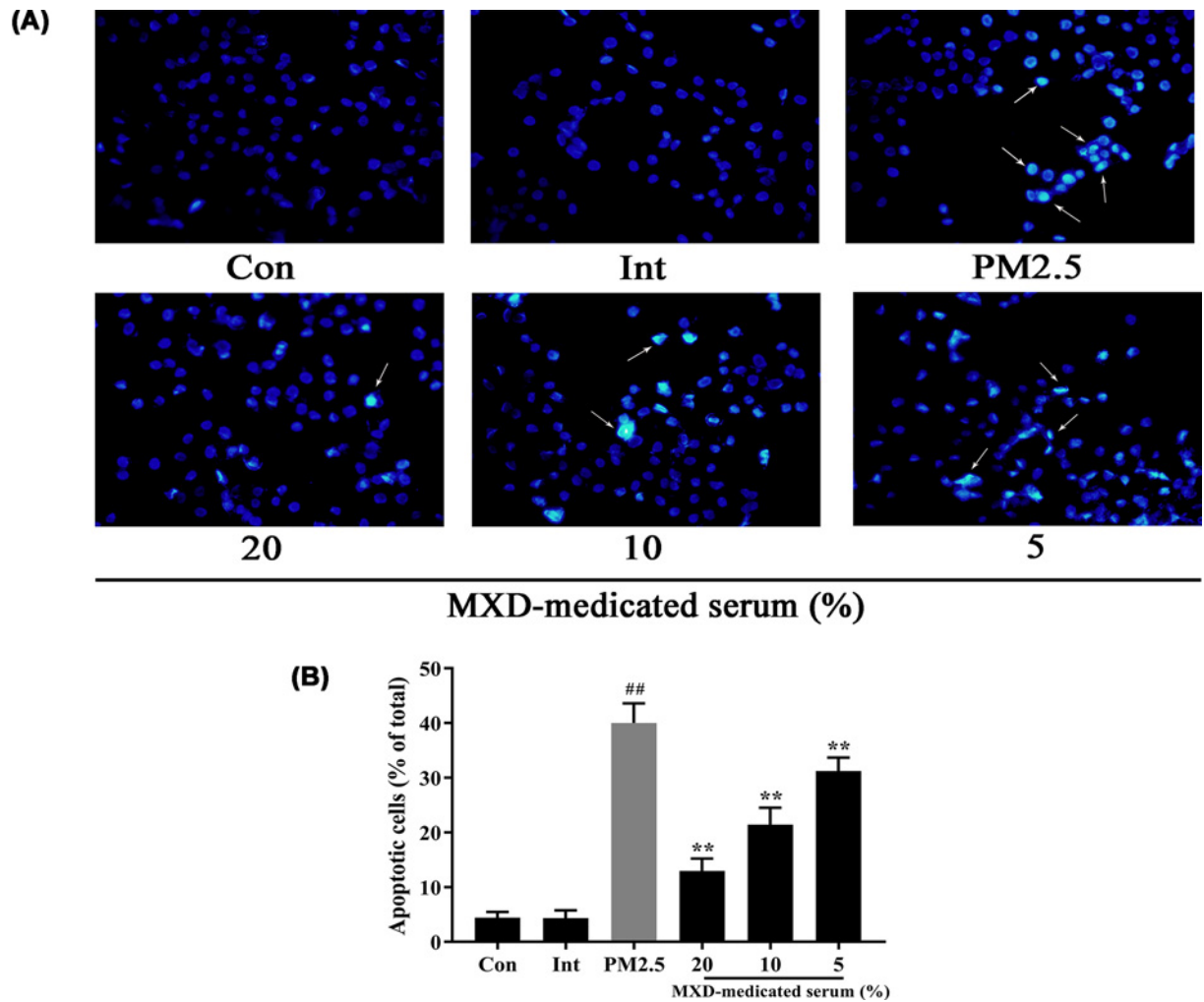


Figure 6. MXD-mediated serum protects against PM2.5-induced cell apoptosis in A549 cells

(A) Changes in nuclear morphology of A549 cells were detected by Hoechst 33253 staining (magnification, $\times 200$). The arrows represent apoptotic cells. (B) Quantitative analysis of the number of apoptotic cells. Data are shown as mean \pm S.D. $n=6$ /group, $**P<0.01$ compared with PM2.5-stimulated group; $\#P<0.01$ compared with control group.

MXD regulated the activation of Akt/mTOR/p70S6K pathway *in vivo* and *in vitro*

For further confirming the molecular pathway mediating the anti-apoptotic effect of MXD, the effect of MXD on the activation of Akt/mTORC1/p70S6K was examined by Western blot both *in vivo* and *in vitro*. As shown in Figure 8, in the PM2.5-stimulated group, the expression of the phosphorylated Akt was significantly down-regulated compared with control group ($P<0.01$). After treatment with MXD (16 g/kg) *in vivo*, the expression of p-Akt, p-mTOR and p-p70S6K were increased significantly compared with PM2.5-stimulated group ($P<0.01$). For *in vitro* assay, treatment with MXD-mediated serum (20 and 10%) significantly increased the phosphorylation of Akt, p-mTOR and p-p70S6K ($P<0.01$) which was in accordance with the results *in vivo*.

Discussion

In the current study, we showed clearly that MXD could eliminate PM2.5 stimulation-induced apoptosis via modulating ratio of Bax/Bcl-2 and up-regulate expression of Akt in a dose-dependent manner both *in vivo* and *in vitro*. The underlying mechanisms appear to be attributable to the activation of the Akt signaling pathway.

MXD has been used to treat lung diseases since ancient times. The clear pharmacological effects of the four herbal medicines in MXD have been confirmed. The pseudoephedrine/ephedrine in Ephedra Herb inhibited the apoptosis

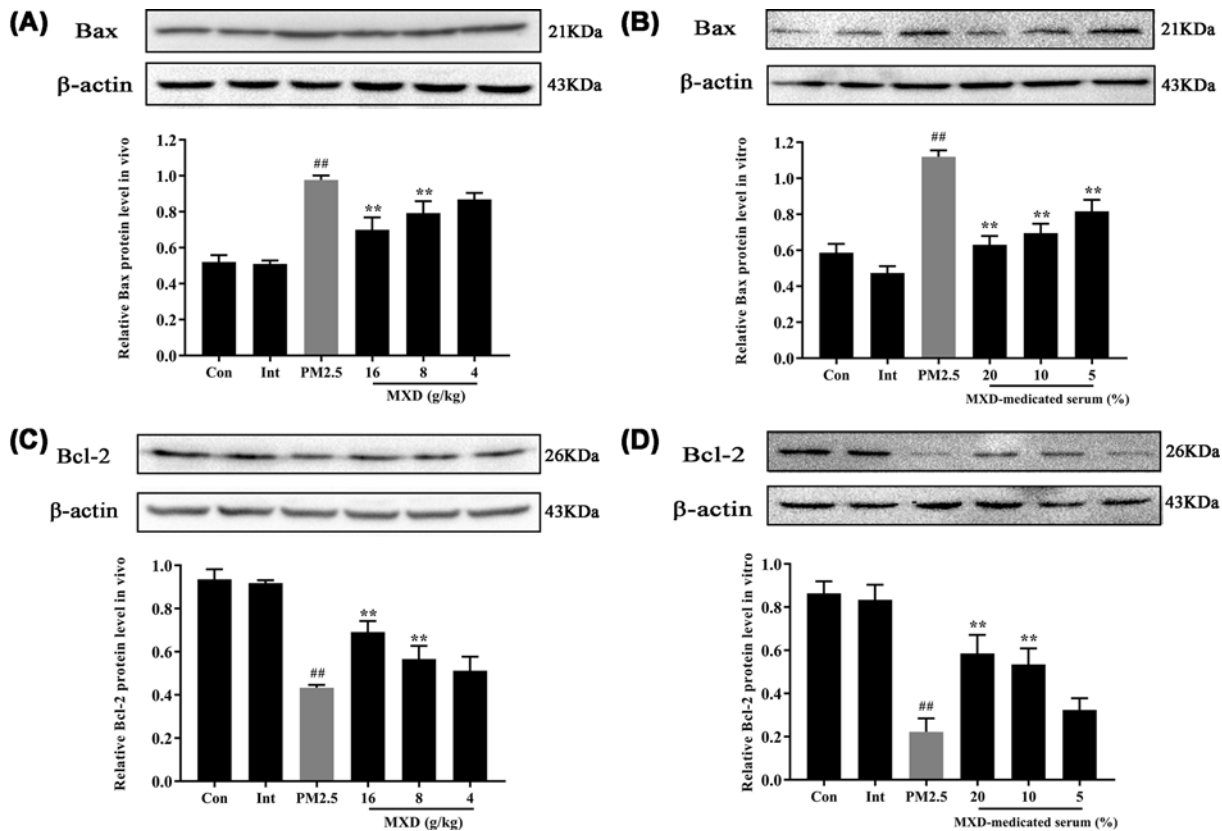


Figure 7. Effect of MXD (or MXD-mediated serum) on Bcl-2 and Bax protein expression in PM2.5-stimulated rats lung tissue and A549 cells

(A) Bax protein expression *in vivo*. (B) Bax protein expression *in vitro*. (C) Bcl-2 protein expression *in vivo*. (D) Bcl-2 protein expression *in vitro*. Data are shown as mean \pm S.D. $n=3$ /group, $**P<0.01$ compared with PM2.5-stimulated group; $##P<0.01$ compared with control group.

of hepatocyte [18]. Liquiritin, a major active component of licorice root, protects mice and HACAT cells from solar ultraviolet B-induced apoptosis [19]. Glycyrrhizic acid ammonium salt is derived from glycyrrhizic acid, which can inhibit hepatocyte apoptosis by regulating the balance of Th cells in the liver [20]. Gypsum can inhibit neurospasm in muscle and bronchus [21]. Bitter Almond has expectorant and antitussive effects. Hence, we hypothesized that MXD may have anti-apoptotic effect in lung tissue, and anti-apoptosis was selected as the entry point for studying the underlying mechanism of MXD.

In the current study, PM2.5-stimulation caused apoptosis both *in vivo* and *in vitro*. After the PM2.5 stimulation, the rats showed symptoms like shortness of breath and nasal cavity effusion. Moreover, TUNEL results also showed a large area of positive cells appeared in lung tissue induced by PM2.5. Furthermore, HE staining in PM2.5-stimulated group shows a serious injury in lung tissue. *In vitro*, after PM2.5 stimulation, the MTT result showed the cell viability was significantly decreased, and Hoechst staining result also showed a large number of apoptotic cells.

In the present study, we investigated whether MXD could display the anti-apoptotic effect as we expected both *in vivo* and *in vitro*. Result of HE staining demonstrated that treatment of MXD could decrease the histopathological lesions' scores effectively after stimulation. The reduction in TUNEL positive cells revealed that treatment of MXD significantly decreased the apoptotic rate in rat lung tissue. To verify the capability of MXD in regulating cell apoptosis after PM2.5 exposure *in vitro*, we evaluated the therapeutic effect of MXD-mediated serum in A549 cells. The results of the MTT assay in A549 cells indicated that MXD-mediated serum could reduce the cell death rate significantly after PM2.5 stimulation. Moreover, the result of Hoechst staining showed that the level of cell apoptosis was decreased after MXD-mediated serum incubation. MXD forcefully prevented the pulmonary cell apoptosis both *in vivo* and *in vitro*, revealing that MXD is an effective drug for protecting lungs from the stimulation of PM2.5.

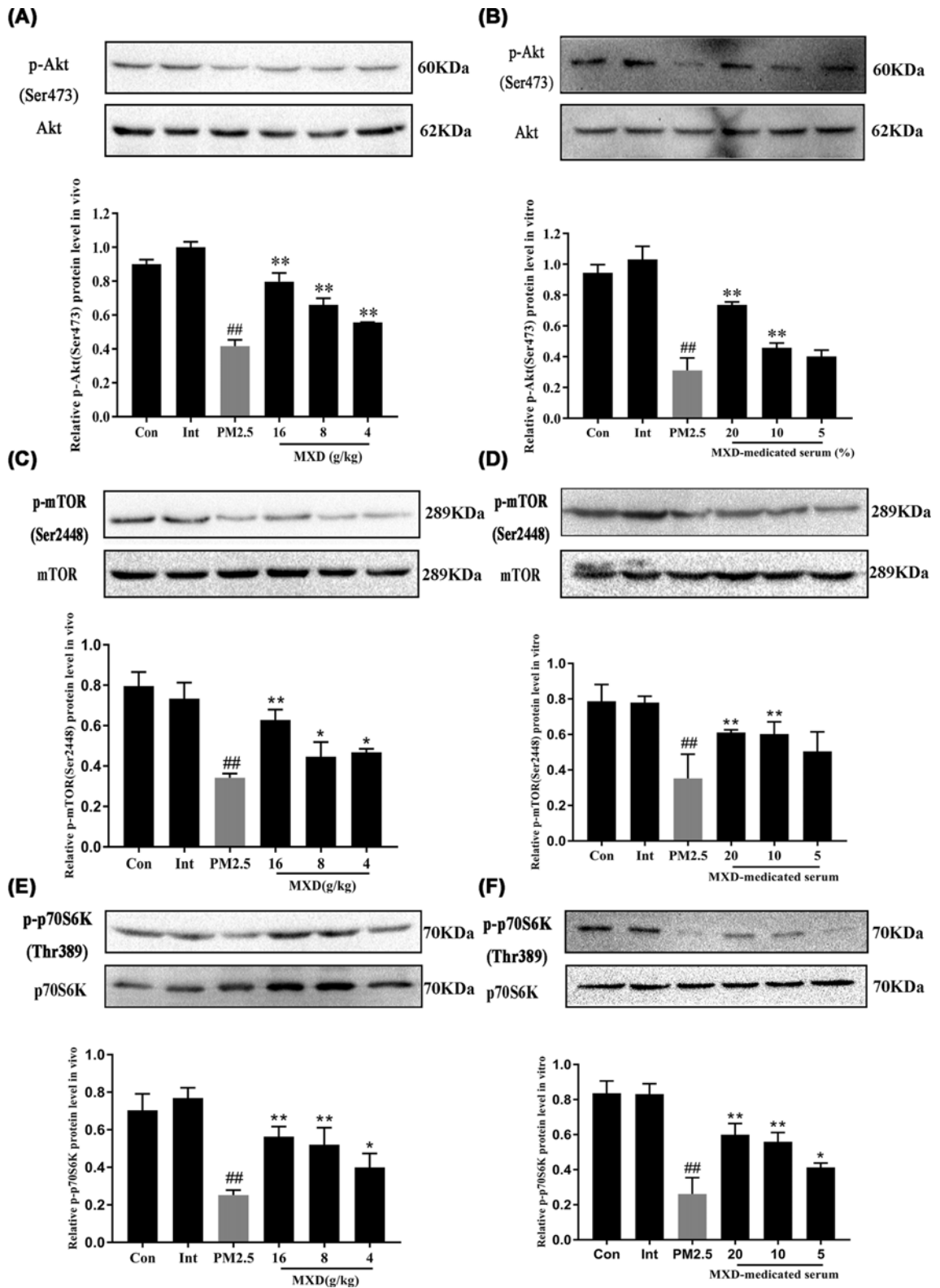


Figure 8. Effect of MXD (or MXD-medicated serum) on phosphorylated Akt, mTOR, P70S6K expressions in PM2.5-stimulated rat lung tissues and A549 cells

(A) *In vivo* p-Akt expression. (B) *In vitro* p-Akt expression. (C) *In vivo* p-mTOR expression. (D) *In vitro* p-mTOR expression. (E) *In vivo* p-p70S6K expression. (F) *In vitro* p-p70S6K expression. Data are expressed as mean \pm S.D. $n=3$ /group, * $P<0.05$, ** $P<0.01$ compared with PM2.5-stimulated group; ## $P<0.01$ compared with control group.

There are two primary mechanisms that mediate apoptosis, the internal pathway and the external death receptor pathway [22]. Among them, the intrinsic pathway, which mediated by mitochondria, plays a central role in the regulation of apoptosis. When cells are stimulated by apoptosis signals, the permeability of mitochondrial outer membrane is changed [23]. In the meantime, apoptosis factors such as Cytc are released into the cytoplasm [24]. Mitochondria is mainly regulated by Bcl-2 family [25]. There are two proteins (Bcl-2 and Bax) of different functions in Bcl-2 family. Bcl-2 is an anti-apoptotic protein, which can maintain the mitochondrial integrity by intercepting Cytc [26,27]. Nevertheless, Bax is a pro-apoptotic protein, which can accelerate the release and delivery of Cytc [28,29]. The Bax/Bcl-2 ratio is also widely used to evaluate the level of apoptosis [30]. Caspase-3 is a potent and common effector of apoptosis. C-caspase-3 (the activated form of Caspase-3) triggers the final process of apoptosis and mediates cell destruction [31], and inhibiting C-caspase3 could block apoptosis [32]. Thus, Cytc and C-caspase-3 can reflect the apoptosis. In the present study, PM2.5 could induce the release of Cytc, activate caspase-3, increase the expression of Bax and decrease the expression of Bcl-2. Our results revealed that administration of MXD could decrease the expression of Cytc and C-caspase-3 in PM2.5-stimulated rat lung. Moreover, our data showed that MXD could reciprocally regulate the expression of Bcl-2 and Bax, proving the anti-apoptotic effects of MXD.

In order to further explore the potential signaling pathways related to the anti-apoptotic effects of MXD, we determined the activation of Akt signaling pathway both *in vivo* and *in vitro*. As an upstream kinase of apoptosis, Akt (also known as protein kinase B, PKB) is important in the regulation of cell survival/apoptosis, proliferation and angiogenesis [33,34]. Several reports have observed that Akt is frequently activated among lung injury in previous years, initiating a series of anti-apoptotic signals [35–37]. Accumulating evidence demonstrates that activation of Akt phosphorylation may regulate apoptosis [38–40]. Activation of PI3K/Akt signaling pathway plays an important role in inhibiting apoptosis [41]. It has been demonstrated that the downstream mTOR plays a critical role in airway inflammation and airway hyperreactivity in asthma [42]. The Akt/mTOR pathway can activate p70S6k to modulate cell growth, migration and apoptosis in various cells [43]. Hence, the activation of Akt/mTOR/p70S6K was examined by Western blotting. In the present study, MXD significantly enhanced the expression of p-AKT (S473), p-mTOR (Ser²⁴⁴⁸) and p-p70S6K (Thr³⁸⁹) *in vivo* and *in vitro*, indicating that MXD may exert anti-apoptotic effect against PM2.5-induced lung injury via activating the Akt/mTOR/p70S6K signaling pathway.

Conclusion

Collectively, MXD could prevent cell apoptosis in a dose-dependent manner via regulating Bcl-2 and Bax expression through the Akt/mTOR/p70S6K pathway. Results of the present study indicate that MXD might be used as an effective agent for the prevention of PM2.5-induced lung injury.

Competing Interests

The authors declare that there are no competing interests associated with the manuscript.

Funding

This work was supported by the 'Key Project of Nanjing Department of Health' [grant number ZKX17047].

Author Contribution

Yunman Li, Weirong Fang and Bo Zhao designed the study. Yefang Wang contributed reagents/materials/funds. Bo Zhao, Yuxiang Fei, Qiyang Yin, Jianping Zhu, Guanghui Ren and Bowen Wang performed the experiments. Bo Zhao and Yuxiang Fei wrote the manuscript.

Acknowledgements

The authors thank Xiao-nan Ma, Min-hui Sun, and Ying-jian Hou for technical support from Cellular and Molecular Biology Center of China Pharmaceutical University.

Abbreviations

Akt/PKB, protein kinase B; Bax, Bcl2-associated x protein; Bcl-2, B-cell lymphoma 2; Cytc, cytochrome c; C-caspase-3, cleaved-caspase-3; DMEM, Dulbecco's modified Eagle's medium; HE, Hematoxylin and Eosin; LSD, least significant difference; MTT, 3-(4,5-dimethylthiazol-2-yl)-2,5-diphenyltetrazolium bromide; MXD, Ma xing shi gan decoction; p70S6K, p70S6 kinase; TUNEL, terminal-deoxynucleotidyl transferase-mediated nick-end labeling; UPLC-MS/MS, ultra-performance liquid chromatography-tandem mass spectrometry/mass spectrometry.

References

- 1 Geng, J., Liu, H., Ge, P., Hu, T., Zhang, Y., Zhang, X. et al. (2019) PM2.5 promotes plaque vulnerability at different stages of atherosclerosis and the formation of foam cells via TLR4/MyD88/NFκB pathway. *Ecotoxicol. Environ. Saf.* **176**, 76–84, <https://doi.org/10.1016/j.ecoenv.2019.03.068>
- 2 Li, J., Li, H., Li, H., Guo, W., An, Z., Zeng, X. et al. (2019) Amelioration of PM2.5-induced lung toxicity in rats by nutritional supplementation with fish oil and Vitamin E. *Respir. Res.* **20**, 76, <https://doi.org/10.1186/s12931-019-1045-7>
- 3 Lin, Y., Zou, J., Yang, W. and Li, C.-Q. (2018) A review of recent advances in research on PM2.5 in China. *Int. J. Environ. Res. Public Health* **15**, 438, <https://doi.org/10.3390/ijerph15030438>
- 4 He, M., Ichinose, T., Yoshida, S., Ito, T., He, C., Yoshida, Y. et al. (2017) PM2.5-induced lung inflammation in mice: differences of inflammatory response in macrophages and type II alveolar cells. *J. Appl. Toxicol.* **37**, 1203–1218, <https://doi.org/10.1002/jat.3482>
- 5 Li, J., Zhou, Q., Yang, T., Li, Y., Zhang, Y., Wang, J. et al. (2018) SGK1 inhibits PM2.5-induced apoptosis and oxidative stress in human lung alveolar epithelial A549 cells. *Biochem. Biophys. Res. Commun.* **496**, 1291–1295, <https://doi.org/10.1016/j.bbrc.2018.02.002>
- 6 Henson, P.M. and Tuder, R.M. (2008) Apoptosis in the lung: induction, clearance and detection. *Am. J. Physiol. Lung Cell. Mol. Physiol.* **294**, L601–L611, <https://doi.org/10.1152/ajplung.00320.2007>
- 7 Lee, F.Y., Lee, M.S., Wallace, C.G., Huang, C.R., Chu, C.H., Wen, Z.H. et al. (2019) Short-interval exposure to ambient fine particulate matter (PM2.5) exacerbates the susceptibility of pulmonary damage in setting of lung ischemia-reperfusion injury in rodent: pharmacomodulation of melatonin. *Biomed. Pharmacother.* **113**, 108737, <https://doi.org/10.1016/j.biopha.2019.108737>
- 8 Liao, Y.H., Li, C.L., Lin, C.C., Lin, J.G., Chiang, J.H. and Li, T.C. (2017) Traditional Chinese medicine as adjunctive therapy improves the long-term survival of lung cancer patients. *J. Cancer Res. Clin. Oncol* **143**, 2425–2435
- 9 Zhong, Y., Zhou, J., Liang, N., Liu, B., Lu, R., He, Y. et al. (2016) Effect of Maxing Shigan Tang on H1N1 Influenza A virus-associated acute lung injury in mice. *Intervirology* **59**, 267–274, <https://doi.org/10.1159/000458726>
- 10 Nair, A.B. and Jacob, S. (2016) A simple practice guide for dose conversion between animals and human. *J. Basic Clin. Pharm.* **7**, 27–31, <https://doi.org/10.4103/0976-0105.177703>
- 11 Guo, Y., Wang, L., Ma, R., Mu, Q., Yu, N., Zhang, Y. et al. (2016) JiangTang XiaoKe granule attenuates cathepsin K expression and improves IGF-1 expression in the bone of high fat diet induced KK-Ay diabetic mice. *Life Sci.* **148**, 24–30, <https://doi.org/10.1016/j.lfs.2016.02.056>
- 12 Li, B., Zeng, M., He, W., Huang, X., Luo, L., Zhang, H. et al. (2015) Ghrelin protects alveolar macrophages against lipopolysaccharide-induced apoptosis through growth hormone secretagogue receptor 1a-dependent c-Jun N-terminal kinase and Wnt/beta-catenin signaling and suppresses lung inflammation. *Endocrinology* **156**, 203–217, <https://doi.org/10.1210/en.2014-1539>
- 13 Yan, Y.Y., Ao, L.Y., Zhou, L., Li, C.Y., Fang, W.R., Shen, W.Y. et al. (2018) Therapeutic effects of JLX001 on cerebral ischemia through inhibiting platelet activation and thrombus formation in rats. *Biomed. Pharmacother.* **106**, 805–812, <https://doi.org/10.1016/j.biopha.2018.07.023>
- 14 Lee, J.Y., Lee, H.E., Kang, S.R., Choi, H.Y., Ryu, J.H. and Yune, T.Y. (2014) Fluoxetine inhibits transient global ischemia-induced hippocampal neuronal death and memory impairment by preventing blood-brain barrier disruption. *Neuropharmacology* **79**, 161–171, <https://doi.org/10.1016/j.neuropharm.2013.11.011>
- 15 Deng, H., Ma, J., Liu, Y., He, P. and Dong, W. (2019) Combining alpha-Hederin with cisplatin increases the apoptosis of gastric cancer in vivo and in vitro via mitochondrial related apoptosis pathway. *Biomed. Pharmacother.* **120**, 109477, <https://doi.org/10.1016/j.biopha.2019.109477>
- 16 Qiu, Y., Yin, Q., Fei, Y., Li, Y., Huang, H., Fang, W. et al. (2019) JLX001 modulated the inflammatory reaction and oxidative stress in pMCAO rats via inhibiting the TLR2/4-NF-κB signaling pathway. *Neurochem. Res* **44**, 1924–1938
- 17 Crowley, L.C., Marfell, B.J. and Waterhouse, N.J. (2016) Analyzing cell death by nuclear staining with Hoechst 33342. *Cold Spring Harb. Protoc.* **2016**, 778–781, <https://doi.org/10.1101/pdb.prot087205>
- 18 Wu, Z., Kong, X., Zhang, T., Ye, J., Fang, Z. and Yang, X. (2014) Pseudoephedrine/ephedrine shows potent anti-inflammatory activity against TNF-α-mediated acute liver failure induced by lipopolysaccharide/d-galactosamine. *Eur. J. Pharmacol.* **724**, 112–121, <https://doi.org/10.1016/j.ejphar.2013.11.032>
- 19 Li, X.Q., Cai, L.M., Liu, J., Ma, Y.L., Kong, Y.H., Li, H. et al. (2018) Liquiritin suppresses UVB-induced skin injury through prevention of inflammation, oxidative stress and apoptosis through the TLR4/MyD88/NFκB and MAPK/caspase signaling pathways. *Int. J. Mol. Med.* **42**, 1445–1459
- 20 Tian, X., Liu, Y., Liu, X., Gao, S. and Sun, X. (2019) Glycyrrhizic acid ammonium salt alleviates Concanavalin A-induced immunological liver injury in mice through the regulation of the balance of immune cells and the inhibition of hepatocyte apoptosis. *Biomed. Pharmacother.* **120**, 109481, <https://doi.org/10.1016/j.biopha.2019.109481>
- 21 Kumasaka, D., Lindeman, K.S., Clancy, J., Lande, B., Croxton, T.L. and Hirshman, C.A. (1996) MgSO4 relaxes porcine airway smooth muscle by reducing Ca²⁺ entry. *Am. J. Physiol.* **270**, L469–L474
- 22 Shi, S., Liu, X. and Li, H. (2017) Downregulation of caspase-3 alleviates Mycoplasma pneumoniae-induced apoptosis in alveolar epithelial cells. *Mol. Med. Rep.* **16**, 9601–9606, <https://doi.org/10.3892/mmr.2017.7782>
- 23 Gibson, C.J. and Davids, M.S. (2015) BCL-2 antagonism to target the intrinsic mitochondrial pathway of apoptosis. *Clin. Cancer Res.* **21**, 5021–5029, <https://doi.org/10.1158/1078-0432.CCR-15-0364>
- 24 Vladimirov, Y.A., Proskurnina, E.V. and Alekseev, A.V. (2013) Molecular mechanisms of apoptosis. structure of cytochrome c-cardiolipin complex. *Biochemistry* **78**, 1086–1097, <https://doi.org/10.1134/S0006297913100027>
- 25 Gupta, R. and Ghosh, S. (2017) Putative roles of mitochondrial Voltage-Dependent Anion Channel, Bcl-2 family proteins and c-Jun N-terminal Kinases in ischemic stroke associated apoptosis. *Biochim. Open* **4**, 47–55, <https://doi.org/10.1016/j.biopen.2017.02.002>
- 26 Cui, J. and Placzek, W.J. (2018) Post-transcriptional regulation of anti-apoptotic BCL2 family members. *Int. J. Mol. Sci.* **19**, 308, <https://doi.org/10.3390/ijms19010308>

- 27 Zheng, J.-H., Xie, L., Li, N., Fu, Z.-Y., Tan, X.-F., Tao, R. et al. (2019) PD98059 protects the brain against mitochondrial-mediated apoptosis and autophagy in a cardiac arrest rat model. *Life Sci.* **232**, 116618, <https://doi.org/10.1016/j.lfs.2019.116618>
- 28 Eldering, E., Mackus, W.J., Derks, I.A., Evers, L.M., Beuling, E., Teeling, P. et al. (2004) Apoptosis via the B cell antigen receptor requires Bax translocation and involves mitochondrial depolarization, cytochrome C release, and caspase-9 activation. *Eur. J. Immunol.* **34**, 1950–1960, <https://doi.org/10.1002/eji.200324817>
- 29 Havasi, A. and Borkan, S.C. (2011) Apoptosis and acute kidney injury. *Kidney Int.* **80**, 29–40, <https://doi.org/10.1038/ki.2011.120>
- 30 Aghdaei, H.A., Kadijani, A.A., Sorrentino, D., Mirzaei, A., Shahrokh, S., Balaii, H. et al. (2018) An increased Bax/Bcl-2 ratio in circulating inflammatory cells predicts primary response to infliximab in inflammatory bowel disease patients. *United Eur. Gastroenterol. J.* **6**, 1074–1081, <https://doi.org/10.1177/2050640618774637>
- 31 Wen, X.-R., Tang, M., Qi, D.S., Huang, X.-J., Liu, H.-Z., Zhang, F. et al. (2016) Butylphthalide suppresses neuronal cells apoptosis and inhibits JNK-Caspase3 signaling pathway after brain ischemia/reperfusion in rats. *Cell. Mol. Neurobiol.* **36**, 1087–1095, <https://doi.org/10.1007/s10571-015-0302-7>
- 32 Wen, X.-R., Tang, M., Qi, D.-S., Huang, X.-J., Liu, H.-Z., Zhang, F. et al. (2016) Butylphthalide suppresses neuronal cells apoptosis and inhibits JNK-Caspase3 signaling pathway after brain ischemia/reperfusion in rats. *Cell. Mol. Neurobiol.* **36**, 1087–1095, <https://doi.org/10.1007/s10571-015-0302-7>
- 33 Kim, A.H., Khursigara, G., Sun, X., Franke, T.F. and Chao, M.V. (2001) Akt phosphorylates and negatively regulates apoptosis signal-regulating kinase 1. *Mol. Cell. Biol.* **21**, 893–901, <https://doi.org/10.1128/MCB.21.3.893-901.2001>
- 34 Wang, B., Luo, Y., Zhou, X. and Li, R. (2018) Trifluoperazine induces apoptosis through the upregulation of Bax/Bcl2 and downregulated phosphorylation of AKT in mesangial cells and improves renal function in lupus nephritis mice. *Int. J. Mol. Med.* **41**, 3278–3286
- 35 Luo, X., Lin, B., Gao, Y., Lei, X., Wang, X., Li, Y. et al. (2019) Genipin attenuates mitochondrial-dependent apoptosis, endoplasmic reticulum stress, and inflammation via the PI3K/AKT pathway in acute lung injury. *Int. Immunopharmacol.* **76**, 105842, <https://doi.org/10.1016/j.intimp.2019.105842>
- 36 Wu, X.T., Ansari, A.R., Pang, X.X., Li, H.Z., Zhang, Z.W., Luo, Y. et al. (2019) Visfatin plays a significant role in alleviating lipopolysaccharide-induced apoptosis and autophagy through PI3K/AKT signaling pathway during acute lung injury in mice. *Arch Immunol Ther Exp (Warsz)* **67**, 249–261
- 37 Li, J., Dou, X., Li, D., He, M., Han, M. and Zhang, H. (2019) Dexmedetomidine ameliorates post-CPB lung injury in rats by activating the PI3K/Akt pathway. *J. Invest. Surg.* **33**, 576–583, <https://doi.org/10.1080/08941939.2018>
- 38 Huang, J., Kodithuwakku, N.D., He, W., Zhou, Y., Fan, W., Fang, W. et al. (2015) The neuroprotective effect of a novel agent N2 on rat cerebral ischemia associated with the activation of PI3K/Akt signaling pathway. *Neuropharmacology.* **95**, 12–21, <https://doi.org/10.1016/j.neuropharm.2015.02.022>
- 39 Nan, F., Sun, G., Xie, W., Ye, T., Sun, X., Zhou, P. et al. (2019) Ginsenoside Rb1 mitigates oxidative stress and apoptosis induced by methylglyoxal in SH-SY5Y cells via the PI3K/Akt pathway. *Mol. Cell. Probes.* **48**, 101469, <https://doi.org/10.1016/j.mcp.2019.101469>
- 40 Jing, Z.T., Liu, W., Xue, C.R., Wu, S.X., Chen, W.N., Lin, X.J. et al. (2019) AKT activator SC79 protects hepatocytes from TNF-alpha-mediated apoptosis and alleviates d-Gal/LPS-induced liver injury. *Am. J. Physiol. Gastrointest. Liver Physiol.* **316**, G387–G396, <https://doi.org/10.1152/ajpgi.00350.2018>
- 41 Chen, L., Wei, X., Hou, Y., Liu, X., Li, S., Sun, B. et al. (2014) Tetramethylpyrazine analogue CXC195 protects against cerebral ischemia/reperfusion-induced apoptosis through PI3K/Akt/GSK3beta pathway in rats. *Neurochem. Int.* **66**, 27–32, <https://doi.org/10.1016/j.neuint.2014.01.006>
- 42 Yang, C.C., Lin, C.C., Hsiao, L.D. and Yang, C.M. (2018) Galangin inhibits thrombin-induced MMP-9 expression in SK-N-SH cells via protein kinase-dependent NF-kappaB phosphorylation. *Int. J. Mol. Sci.* **19**, 4084, <https://doi.org/10.3390/ijms19124084>
- 43 Zhang, Q., Qiao, H., Wu, D., Lu, H., Liu, L., Sang, X. et al. (2019) Curcumin potentiates the galbanic acid-induced anti-tumor effect in non-small cell lung cancer cells through inhibiting Akt/mTOR signaling pathway. *Life Sci.* **239**, 117044, <https://doi.org/10.1016/j.lfs.2019.117044>

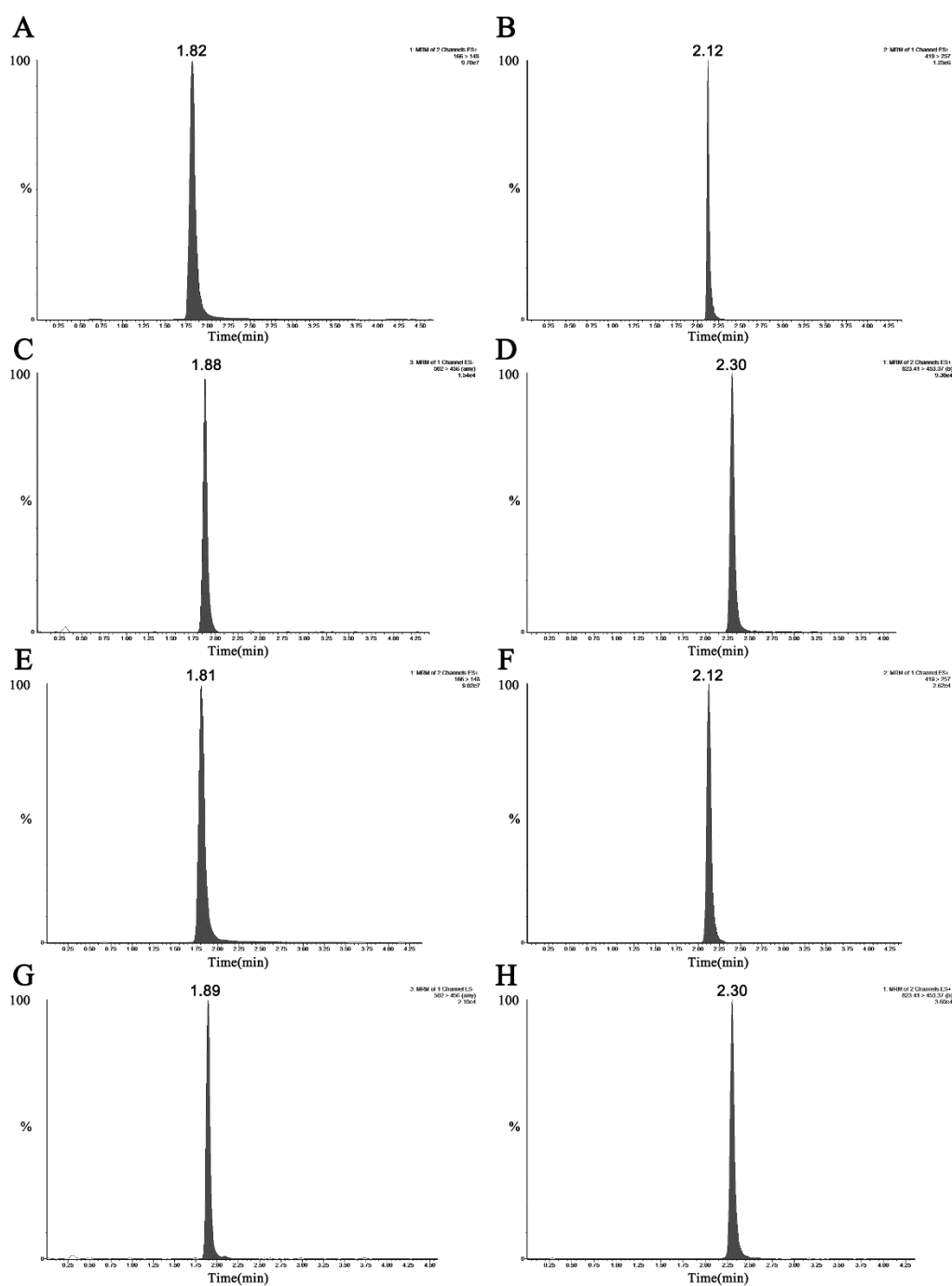


Figure S1. Representative chromatograms of the five compounds in reference standard solution and medicated serum. (A) Representative chromatograms of ephedrine (500 ng/mL) and pseudoephedrine (500 ng/mL) in standard solution. (B) Representative chromatogram of liquiritin (500 ng/mL) in standard solution. (C) Representative chromatogram of glycyrrhizic acid (500 ng/mL) in standard solution. (D) Representative chromatogram of amygdalin (500 ng/mL) in standard solution. (E) Representative chromatograms of ephedrine and pseudoephedrine in medicated serum. (F) Representative chromatogram of liquiritin in medicated serum. (G) Representative chromatogram of glycyrrhizic acid in medicated serum. (H) Representative chromatogram of amygdalin in medicated serum.

Supplementary materials

Ma xingshigan Decoction (MXD) eliminates PM2.5-induced lung injury by reducing pulmonary cell apoptosis through Akt/mTOR/p70S6K pathway in rats

Yefang Wang^{1a}, Bo Zhao^{2a*}, Yuxiang Fei², Qiyang Yin², Jianping Zhu², Guanghui Ren², Bowen Wang², Weirong Fang^{2*}, Yunman Li^{2*}

Department of Paediatrics, Nanjing Integrated Traditional Chinese and Western Medicine Hospital, Nanjing 210014, PR China.

² State Key Laboratory of Natural Medicines, School of Basic Medicine and Clinical Pharmacy, China Pharmaceutical University, Nanjing 210009, PR China

* Corresponding author1: Bo Zhao. E-mail: 532045956@qq.com;

* Corresponding author2: Weirong Fang. E-mail: weirongfang@163.com;

* Corresponding author 3: Yunman Li. E-mail: yunmanlicpu@163.com.

^aThese two authors contributed equally to this study.

Analysis of the medicated serum

After collecting the medicated serum, 250 μ L precipitant (Acetonitrile/Methanol, v/v, 1:1) was added to 50 μ L rat plasma sample. The mixture was vortex-mixed for 10 min, centrifuged at 8°C for 10 min at 15000 rpm, and 2 μ L of the supernatant was injected into a column for analysis.

The quantification of ephedrine (and pseudoephedrine), liquiritin, glycyrrhizic acid and amygdalin was conducted using external standard method with a UPLC-MS/MS system. The UPLC separation was performed at 50 °C using an Acquity UPLC HSS T3 (2.1 \times 30 mm, 1.8 μ m) column. Mobile phase solvent A was consisted of aqueous phase of ammonium acetate in concentration 5 mmol/L, and mobile phase solvent B was pure methanol. Positive ionization electrospray MS was employed for ephedrine (and pseudoephedrine), liquiritin and glycyrrhizic acid. Negative ionization electrospray MS was employed for amygdalin. The injection volume was 2 μ L, and gradient elution conditions are shown in Table S1. The optimal instrument conditions, precursor-product ion combination of m/z for each ingredient were shown in Table S2.

Table S1. Elution condition for UPLC-MS/MS analysis of medicated serum

Time (min)	MP A%	MP B%	Flow rate (mL/min)
Initial	96.00	4.00	
1.00	96.00	4.00	
3.50	30.00	70.00	0.500
4.50	30.00	70.00	
4.60	96.00	4.00	
5.00	96.00	4.00	

Table S2. Optimal instrument conditions

Ingredient	Cone (V):	Collision (eV)	Combination of m/z
Ephedrine and Pseudoephedrine	30	12	166.00 \rightarrow 148.00
Liquiritin	42	8	419.00 \rightarrow 257.00
Glycyrrhizic acid	42	8	823.41 \rightarrow 453.37
Amygdalin	30	12	502.00 \rightarrow 456.00

Quantification of main ingredient in the medicated serum

The representative chromatograms of the five compounds in reference standard solution and medicated serum were shown in Figure S1. The concentration of main ingredients of interest were shown in Table S3.

Table S3. The concentration of main ingredients in medicated serum

Ingredient	Concentration (ng/mL)
Ephedrine and pseudoephedrine	925.8
Liquiritin	13.6
Glycyrrhizic acid	203.4
Amygdalin	519.3